Angewandte Chemie

Eine Zeitschrift der Gesellschaft Deutscher Chemiker

Supporting Information

Supporting information to *Angew. Chem. Int. Ed.*

Coencapsulation of Arsenic- and Platinum-based Drugs for Targeted Cancer Treatment

Haimei Chen,[†] Samuel Pazicni,[¶] Nancy L. Krett,[⊤] Richard W. Ahn,[†] James E. Penner-Hahn,[¶] Steven T. Rosen,[⊤] and Thomas V. O'Halloran[†, *]

[†]Chemistry of Life Processes Institute, Northwestern University, Evanston IL 60208, [¶]Department of Chemistry and Biophysics, University of Michgan, Ann Arbor, MI 48109, [⊤]and Robert H. Lurie Comprehensive Cancer Center, Feinberg School of Medicine, Northwestern University, Chicago, IL 60611

Content:
Experimental (liposome preparation, drug release, cytotoxicity assay, confocal microscopy, cellular uptake, analysis of arsenic and platinum complexes)

Figures S1-11
Tables S1-5

Experimental

Materials
Dipalmitoylphosphatidylcholine (DPPC), dioleoylphosphatidylglycerol (DOPG) and 1,2-Dipalmitoyl-*sn*-glycero-3-phosphoethanolamine-*N*-(Lissamine rhodamine B sulfonyl) (ammonium salt) (DPPE-Rh) were purchased from Avanti Polar Lipids (Alabaster, AL, USA). 1,2-Distearoyl-*sn*-glycero-3-phosphoethanolamine-*N*-[folate(polyethylene glycol)-3350] (DSPE-PEG$_{3350}$-Folate) was synthesized according to the literature.[1] Cholesterol (Chol), arsenic trioxide (As_2O_3), sodium arsenite ($NaAsO_2$), cisplatin (cisPt), silver acetate (Ag(OAc)), folic acid (FA), paraformaldehyde, 2-[4-(2-hydroxyethyl)-1-piperazine]ethanesulfonic acid (HEPES), 2-[*N*-Morpholino]ethanesulfonic acid (MES), Bicine, sucrose, sodium dodecyl sulfate (SDS), phenazine methosulfate (PMS), human insulin solution, and Sephadex G50 were obtained from Sigma-Aldrich (St. Louis, MO, USA). Sodium nitrate was from Mallinckrodt (Kentucky, USA). 3-(4,5-dimethylthiazol-2-yl)-5-(3-carboxymethoxyphenyl)-2-(4-sulfophenyl)-2*H*-tetrazolium (MTS) was from Promega (Madison, WI, USA). RPMI-1640, folate-deficient RPMI-1640, fetal bovine serum (FBS) were from INVITROGEN-GIBCO (Carlsbad, CL, USA). Charcoal dextran–stripped fetal bovine serum (cds-FBS) was from Atlanta Biologicals, Inc. (Lawrenceville, GA, USA). Eagle's Minimum Essential Medium (EMEM) was from the American Type Culture Collection (ATCC) (Manassas, VA, USA). *L*-Glutamine, penicillin-streptomycin, and phosphate-buffered saline (PBS) were from MEDIATECH (Herndon, VA, USA). Amphotericin B from Biologas (Montgomery, IL, USA).

Coencapsulation of Arsenic- and Platinum-based Drugs within Liposomes

(a) Preparation of aqua-cisPt gradients
The acetate solution of aqua-cisPt (300 mM [*cis*-$(NH_3)_2Pt(OH_2)_2$](OAc)$_2$) was prepared as previously reported.[2] Briefly, 360 mg cisPt (*cis*-$(NH_3)_2PtCl_2$) was mixed with 370 mg Ag(OAc) in 4 mL MQ-H_2O at 50ºC in the dark for 4-5 h. The mixture was then kept at 20ºC overnight before filtered through a 0.2 μm syringe filter (cellulose acetate membrane, Nalgene) to remove the white AgCl precipitate. The obtained pale yellow solution (pH 5.1) was sealed and kept at 4ºC in the dark and used within two weeks.

Lipid mixtures of DPPC/DOPG/Chol with various molar ratios (51.4/3.6/45, 86.4/3.6/10, and 96.4/3.6/0) were dissolved in chloroform. For rhodamine (Rh)-labeled liposomes, 0.5% DPPE-Rh was included. The chloroform was then removed by rotary vacuum evaporation to form lipid film on the vial, which was subsequently placed under a high vacuum overnight to remove any residual solvent. The dried lipid film was hydrated in 300 mM aqua-cisPt acetate (Figure S1a) to form multilamellar vesicles (MLVs), which were further subjected to 7 freeze-and-thaw cycles (freezing in a ethanol/dry-ice bath and thawing in a water bath at 50ºC).[3] The liposomes were then extruded with a manual mini-extruder (Avanti Lipids, AL, USA), 10 times through two stacked polycarbonate

filters of 0.1 μm pore size at 40ºC. Extruded liposomes in the aqua-cisPt acetate were then fractionated on Sephadex G-50 columns (1 mL sample volumes were placed on columns with at least a 20 mL column bed) equilibrated with the buffer of 300 mM sucrose (or NaNO$_3$), 10 mM MES, pH 5.1 (Figure S1b).
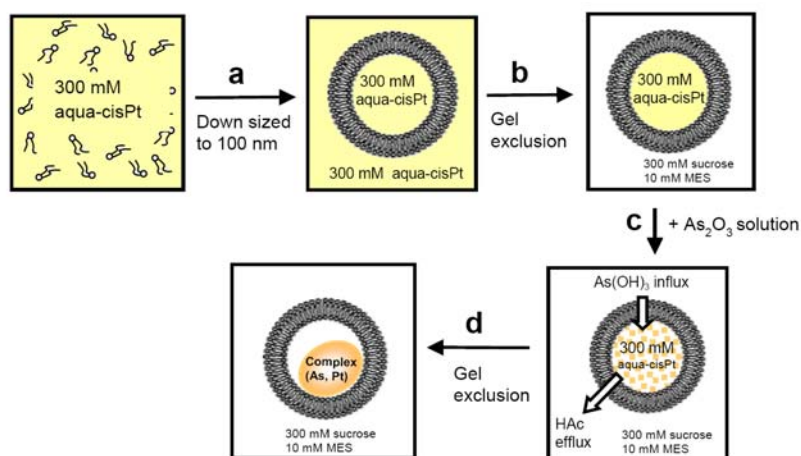

Figure S1. The procedure of coencapsulating arsenic- and platinum-based drugs into liposomes. (a) Hydration of dried lipids in 300 mM aqua-cisPt acetate (pH 5.1). Self-assembled liposomes are then reduced to 100 nm by extrusion. (b) Gel exclusion for exchanging external buffer into 300 mM sucrose, 10 mM MES, pH 5.1. (c) Liposome suspension is added with As$_2$O$_3$ solution and kept at 50°C and pH 6.6-6.9 for 11 h. (d) The influx of As(OH)$_3$ into liposomes to form complex(As, Pt), accompanied by the efflux of acetate acids (HAc). Removal of excess of external As(OH)$_3$ by gel exclusion with 300 mM sucrose, 10 mM MES, pH 7.4-8.0, followed by adjusting the pH of final liposome product back to 6.1-6.4.

(b) Arsenic loading. Typically, for 30 mg of DPPC/DOPG/Chol, 51.4/3.6/45 mol%, after removal of extraliposomal platinum species using the Sephadex G-50 column (Figure S1b), 180 μL of arsenic trioxide solution (As 300 mM) was added to these aqua-cisPt acetate-containing liposomes at an initial As/lipid molar ratio of ~4 and a lipid concentration of ~5 mM, and the pH of mixture was adjusted to 6.6-6.9 (Figure S1c). Samples were incubated at 50ºC with frequent vortexing. At various time points, 100 μL aliquots were passed through Sephadex G-50 with the same buffer at pH 7.4-8.0 to remove unencapsulated arsenic and platinum species. The concentrations of lipids (P) and of encapsulated As and Pt in the excluded fractions were determined with an inductively coupled plasma optical emission spectrometer (ICP-OES) (Vista MPX, USA).[4] The molar ratios of As/lipid, Pt/lipid and As/Pt were calculated and used to assess extent of loading at each time point.

Figure 1c shows the dependence of As/lipid, Pt/lipid, and As/Pt molar ratios as a function of incubation time during arsenic loading into liposomes at 50ºC in response to the transmembrane gradient of aqua-cisPt acetate. The As/lipid molar ratio rapidly increased within the first 3 h indicating rapid arsenic loading, and achieved equilibrium after 11 h at molar ratios of As/lipid = 0.66 and As/Pt = 1.4 and a half-time of 40 min.

Figure S2 shows that the extent of arsenic loading into liposomes increased with increasing concentration of intraliposomal aqua-cisPt acetate. When 100 mM aqua-cisPt acetate was used as the intraliposomal media, a value for As/lipid (mol) = 0.27 was obtained after 11 h, compared with the As/lipid (mol) = 0.66 in the case of 300 mM aqua-cisPt acetate.
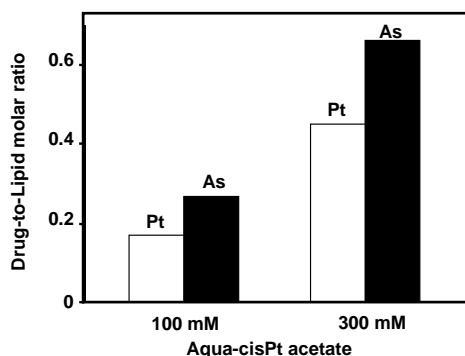
Figure S2. Arsenic-loading extent is dependent on the concentration of intraliposomal aqua-cisPt acetate. DPPC/DOPG/Chol = 51.4/3.6/45 mol%; outer buffer: 120 mM or 300 mM sucrose, 10 mM MES, pH 6.7, 50ºC for 11 h, with an initial As-to-lipid molar ratio of 4.0.

(c) Determination of intraliposomal drug concentration. The kinetics of arsenic loading into 100-nm-liposomes using 300 mM aqua-cisPt acetate as the intraliposomal medium revealed little reduction in the Pt/lipid molar ratio during the loading period of 11 h at 50ºC (Figure 1c). This indicates that the platinum species are efficiently retained inside the liposomes and that little leakage occurred (< 10%). The molar ratio of Pt/lipid 0.48 ± 0.06 (n = 7) at 11 h can be assumed to correspond to 300 mM platinum species within one single liposome of NB(As, Pt). We further found that As/Pt = 1.3 ± 0.1 (n = 7), indicating intraliposomal As = 390 ± 30 mM (n = the number of independent experiments). These values are close to those expected for an encapsulated volume of 1.5 L/mol phospholipid.[5] The mean sizes of NB(As, Pt) were determined as 112 ± 9 nm by dynamic light scattering on a Zetasizer Nano ZS (Malvern Instruments, Malvern, UK). The average intraliposomal core of NB(As, Pt) can be assumed as a sphere with a diameter of ~100 nm and a volume of 5.23×10^{-19} L, considering that the thickness of a lipid bilayer is 4-6 nm.[6, 7] Thus, there are $\sim 12 \times 10^4$ As atoms and $\sim 9 \times 10^4$ Pt atoms per liposome in NB(As, Pt).

Transmission Electron Microscopy (TEM)
Liposome samples were stained with 2% uranyl acetate on 400-mesh copper grids (carbon-coated and formvar-covered, Ted Pella, Inc., USA), and air-dried overnight before TEM analysis at 200 kV, magnification 40,000 $\times$ (Hitachi HF2000, Hitachi High-Technologies, Japan). For visualization of the inorganic cores within the liposomes, some liposome samples were left unstained to avoid the influence of the electron density of uranyl acetate.[4, 8, 9] These unstained samples were analyzed for arsenic and platinum components within the liposomal cores by energy-dispersive X-ray analysis (EDX) (Figure 2).

Stability of Arsenic and Platinum Liposomes
Liposome stability was evaluated with a drug release assay. NB(As, Pt) samples were kept at 4ºC or 37ºC at different pHs with 1 mM lipid. An extraliposomal buffer of 300 mM sucrose (or NaNO₃) and 10 mM MES was used for maintaining the pH at 5.0 and 6.1; for pH 7.4 and 8.2, 20 mM Bicine was additionally added; and for pH 4.0, 20 mM acetic acid was additionally added. The pH of these dispersions were re-adjusted to the indicated values with HNO₃ or NaOH solution. For serum samples, NB(As, Pt) were mixed with FBS in a volume/volume ratio of 2:8 (80% serum) with 1 mM lipid and kept at 37ºC. At various time points, aliquots were passed over a Sephadex G-50 column to remove arsenic and platinum species which had leaked from liposomes. The excluded volume fractions containing liposomes were digested with concentrated HNO₃ (trace metal grade, Fisher Scientific) before ICP-OES analysis for determination of the drug-to-lipid molar ratios. The drug release percentage was calculated as $[(r_o - r_i)/r_o] \times 100\%$, where r_o is the initial drug-to-lipid molar ratio and r_i the drug-to-lipid molar ratio at a specific time point.[4] The results are compared in Figures 3, S3 and S4.

Figure S3 shows stable encapsulation of NB(As, Pt) (DPPC/DOPG/Chol = 51.4/3.6/45 mol%) with little arsenic and platinum release (< 5%) within the range of pH 4.0-8.2 after 3 days at 37ºC.

Figure S4 compares drug release of NB(As, Pt) in serum with three lipid compositions: DPPC/DOPG/Chol = 51.4/3.6/45 mol% (**a**), 86.4/3.6/10 mol% (**b**), and 96.4/3.6/0 mol% (**c**), and their cytotoxic effects on SU-DHL-4 and MDA-MB-231 cells.
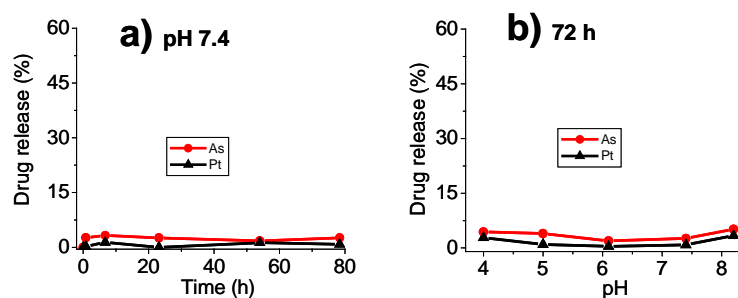
Figure S3. Drug release of NB(As, Pt) at 37ºC as a function of time at pH 7.4 (a) and after 72 h at various pHs (b). DPPC/DOPG/Chol = 51.4/3.6/45 mol%.
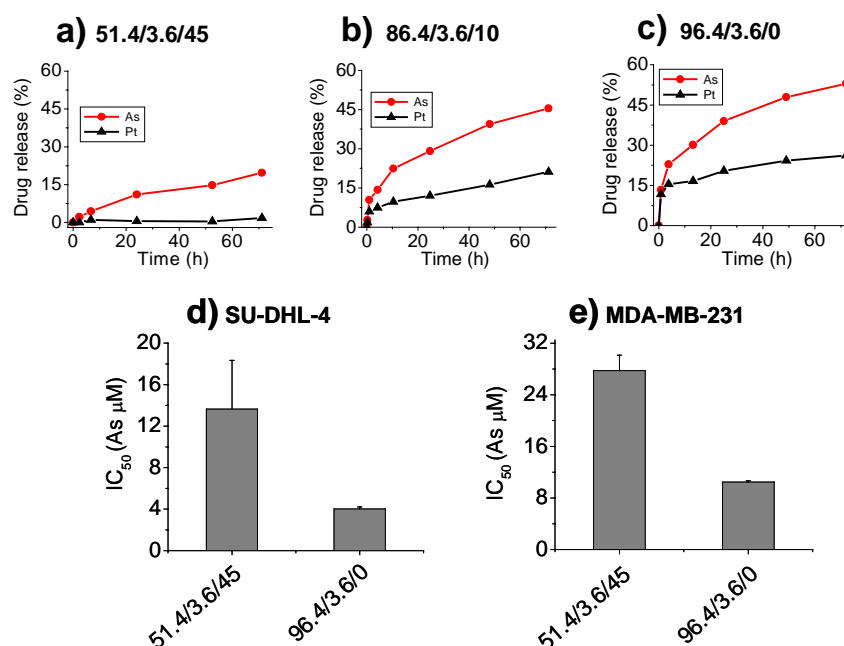

Figure S4. Comparison of drug release of NB(As, Pt) at 37ºC in 80% FBS with various lipid compositions: DPPC/DOPG/Chol = 51.4/3.6/45 (a), 86.4/3.6/10 (b), 96.4/3.6/0 (c), mol%. The faster drug release results in the higher cytotoxic effects (IC_{50}) on SU-DHL-4 (d, 72 h) and MDA-MB-231 cells (e, 96 h).

Preparation of Folate-targeted Arsenic and Platinum Liposomes

The folate-targeting ligand, DSPE-PEG$_{3350}$-Folate, was incorporated into the lipid bilayer of pre-formed NB(As, Pt) using the "post-insertion" technique.[10] Typically, 20 μL of DSPE-PEG$_{3350}$-Folate (5 mg/mL chloroform solution) was placed in a glass tube and the chloroform was removed by rotary evaporation. The resultant lipid film was subsequently placed under a high vacuum overnight to remove any residual solvent. To this dry lipid film was added a suspension of pre-formed NB(As, Pt) (mean size 112 ± 9 nm) at a molar ratio of folate/lipid = 0.7%, in 300 mM sucrose, 10 mM MES, pH 6.4. The mixture was kept at 50ºC for 1.5 h with stirring and then passed through a Sepharose CL-4B column to remove any leaked drugs and unincorporated DSPE-PEG$_{3350}$-Folate. The obtained folate-targeted liposomes (f-NB(As, Pt)) were analyzed by ICP-OES for arsenic, platinum and lipid concentrations, yielding molar ratios of 0.59 ± 0.01 for As/lipid and 0.48 ± 0.02 for Pt/lipid. The mean liposome diameters were determined as 129 ± 4 nm by dynamic light scattering on a Zetasizer Nano ZS (Malvern Instruments, Malvern, UK), 17 nm larger than those of NB(As, Pt). The folate content of f-NB(As, Pt) preparations was determined by lysing the liposomes with 5% SDS and measuring the UV absorbance at 285 nm.[11] All samples in 5% SDS were prepared in a 96-well half-area microplate (Greiner Bio-one GmbH, Germany), 150 μL per well. To ensure every well had the same background, standard solutions (0-0.4 μM free folate acid (FA)) were additionally mixed with NB(As, Pt) at the same lipid level as in f-NB(As, Pt). The plate was then kept in the dark for 24-48 h and centrifuged at 500 g, 5-10 min (to eliminate bubbles) before reading the absorbance at 285 nm. Figure S5 is a

typical standard curve of FA absorbance vs. concentration in the presence of 0.5 mM lipids from NB(As, Pt) and 5% SDS. The FA concentration of f-NB(As, Pt) was derived from the standard curve, giving the molar ratio of 0.56 (± 0.15)% folate/lipid.
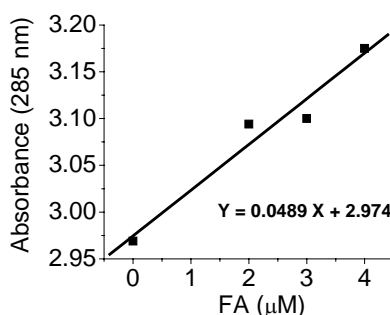

Y = 0.0489 X + 2.974

Figure S5. Standard curve of FA absorbance at 285 nm vs. concentration in aqueous solution in the presence of 0.5 mM lipids from NB(As, Pt) and 5% SDS.

Cell Culture

SU-DHL-4 (human lymphoma B cells) was from the Deutsche Sammlung von Mikroorganismen und Zellkulturen GmbH (DSMZ, Braunschweig, Germany). MM.1S (human multiple myeloma B cells) was previously established in one of our laboratories (N. L. Krett and S. T. Rosen). IM-9 (human lymphoblast B cells), MDA-MB-231 (human breast adenocarcinoma cells), OVCAR-3 (human ovary adenocarcinoma cells), KB (human nasopharyngeal epidermal carcinoma cells, FR$^+$), and MCF-7 (human breast carcinoma cells, FR$^-$)[12, 13] were purchased from ATCC (Manassas, VA, USA).

All Cells were maintained at 37ºC in an incubator with 5% CO_2 and harvested in the exponential phase of growth. SU-DHL-4, IM-9, and MM.1S cells were cultured in RPMI-1640 supplemented with 10% FBS, 2 mM glutamine, 100 units/mL penicillin-streptomycin, and 2.5 µg/mL Amphotericin B. MDA-MB-231 cells were cultured in DMEM/F12 supplemented with 5% cds-FBS, 2 mM glutamine, 100 units/mL penicillin-streptomycin, and 0.1% human insulin solution. OVCAR-3 cells were cultured in RPMI-1640 supplemented with 20% FBS, 100 units/mL penicillin-streptomycin, and 0.1% human insulin solution. MCF-7 cells was cultured in EMEM supplemented with 10% FBS, 2 mM glutamine, 100 units/mL penicillin-streptomycin and 2.5 µg/mL Amphotericin B. KB cells were cultured in EMEM supplemented with 10% FBS and 50 units/mL penicillin-streptomycin. For folate-targeting experiments, KB cells were transferred into folate-deficient RPMI-1640 medium for more than one week before each experiment.[14]

Cytotoxicity

(a) MTS assay. The *in vitro* cytotoxicities of NB(As, Pt), NB(Pt), As_2O_3, aqua-cisPt acetate and cisPt were determined using the MTS cell proliferation assay as described previously.[15] Briefly, SU-DHL-4 and IM-9 (40,000 cells/mL), and MM.1S (250,000 cells/mL) were treated with drugs and plated in quadruplicate (100 µL/well) onto 96-well plates. For MDA-MB-231 and OVCAR-3, 20,000 cells/mL were plated in quadruplicate (100 µL/well) onto 96-well plates, incubated overnight and then treated with drugs. After incubation for the indicated period at 37ºC, the MTS/PMS solution (20 µL/well) was added to each well and the plates were further incubated for 4 h at 37ºC before reading the absorbance at 490 nm. Cell growth rates were expressed as a function of drug concentration on a logarithmic scale. The IC_{50} values (the drug concentration required for 50% inhibition of cell growth) were determined by fitting to a sigmoidal dose-response curve using Origin 6.0 software (Microcal Software, Inc., Northampton, USA). In the case of the 1.5 h (Figure S6b) or 2 h (Figure S7b) time periods, the cells treated with drugs were first incubated for 1.5 h or 2 h at 37ºC, then washed twice with PBS to remove un-associated drugs or liposomes, and further incubated up to 48 h (Figure S6b) or 72 h (Figure S7b) in drug-free medium, followed by the MTS assay. The data are shown in Tables 1 and S1, and Figures S6-8.

Figure S6 shows that for SU-DHL-4 cells, after a 48-h incubation, NB(As, Pt) (IC_{50} 20.6 µM As or 15.6 µM Pt) exhibited attenuated cytotoxicity relative to the free drugs As_2O_3 (3.7 µM As), aqua-cisPt (5.5 µM Pt) and cisPt (3.5 µM Pt). Notably, NB(As, Pt) was three times more cytotoxic than NB(Pt) (42.4 µM Pt), indicating the bioavailability of both arsenic and platinum species from NB(As, Pt). At long incubation times (> 48 hrs, i.e.), the

cytotoxicities of NB(Pt, As) increased greatly, approaching those of As$_2$O$_3$, aqua-cisPt and cisPt (Figure S6b), consistent with gradual release of the drugs at 37ºC in serum (Figure 3b).
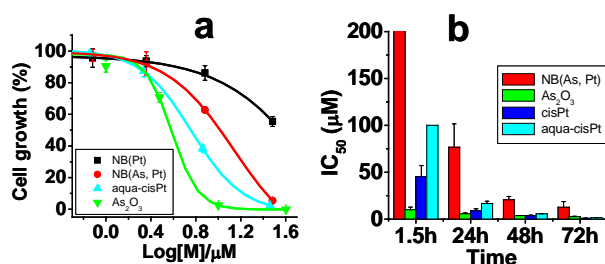

Figure S6. (a) Cytotoxic effects of NB(As, Pt), NB(Pt), aqua-cisPt and As$_2$O$_3$ on SU-DHL-4 cells after a 48 h incubation. For NB(As, Pt), NB(Pt), and aqua-cisPt, M = Pt; for As$_2$O$_3$, M = As. (b) Cytotoxicities (IC$_{50}$) of NB(As, Pt), As$_2$O$_3$, cisPt, and aqua-cisPt after incubation for 1.5 h, 24 h, 48 h, and 72 h. DPPC/DOPG/Chol = 51.4/3.6/45 mol%.
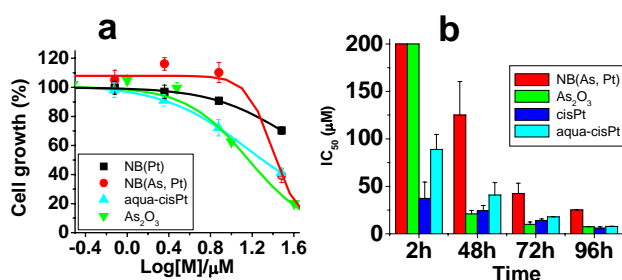

Figure S7. (A) Cytotoxic effects of NB(As, Pt), NB(Pt), aqua-cisPt, and As$_2$O$_3$ on MDA-MB-231 cells after a 72 h incubation. For NB(As, Pt), NB(Pt) and aqua-cisPt, M = Pt; for As$_2$O$_3$, M = As. (C) Cytotoxicities (IC$_{50}$) of NB(As, Pt), As$_2$O$_3$, cisPt, and aqua-cisPt after incubation for 2 h, 48 h, 72 h, and 96 h. DPPC/DOPG/Chol = 51.4/3.6/45 mol%
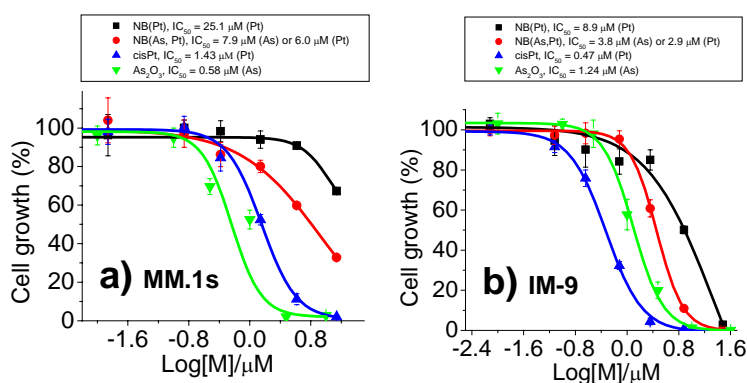

Figure S8. Cytotoxic effects of NB(As, Pt), NB(Pt), cisPt and As$_2$O$_3$ on MM.1S (a) and IM-9 (b) cells after a 72 h incubation. For NB(As, Pt), NB(Pt), and cisPt, M = Pt; for As$_2$O$_3$, M = As. DPPC/DOPG/Chol = 51.4/3.6/45 mol%

Figure S7 shows that for MDA-MB-231 cells, after a 72 h incubation, NB(As, Pt) (IC$_{50}$ 35.0 μM As or 26.6 μM Pt) exhibited attenuated cytotoxicity relative to the free drugs As$_2$O$_3$ (10.0 μM As), aqua-cisPt (17.9 μM Pt) and cisPt (14.0 μM Pt). Notably, NB(As, Pt) was 7 times more cytotoxic than NB(Pt) (> 200 μM Pt), indicating the bioavailability of both arsenic and platinum species from NB(As, Pt). At long incubation times (> 72 hrs, i.e.), the cytotoxicities of NB(As, Pt) increased greatly, approaching those of As$_2$O$_3$, aqua-cisPt and cisPt (Figure S7b), consistent with gradual release of the drugs at 37ºC in serum (Figure 3b).

Similar anticancer activities of NB(As, Pt) were observed for other lymphoma (IM-9), multiple myeloma (MM.1S), and ovary cancer (OVCAR-3) cells (Figure S8, Tables 1 and S1), with NB(As, Pt) being 3-7 times more cytotoxic than NB(Pt).

Table S1. Comparison of cytotoxicities (IC_{50}) of aqua-cisPt and cisPt towards human tumor cells

Cell lines[a]	IC_{50} (Pt/μM)[b]	
	Aqua-cisPt	CisPt
SU-DHL-4	5.5 $\pm$ 0.4	3.5 $\pm$ 0.8
IM-9	1.0 $\pm$ 0.01	0.6 $\pm$ 0.2
MDA-MB-231	17.9 $\pm$ 0.1	14.0 $\pm$ 1.8
OVCAR-3	2.6 $\pm$ 0.8	2.0 $\pm$ 0.01

[a] 48 h-drug treatment for SU-DHL-4 and IM-9, and 72 h-drug treatment for MDA-MB-231 and OVCAR-3 cells. [b] IC_{50} ($\pm$ SD) values are based on two independent experiments.

(b) Guava ViaCount assay
Note: The MTS assay is one of most high throughput and economical assays for detecting viability of cancer cells.[15] In the case of treatment with f-NB(As, Pt), however, it appeared that the folate moiety interfered with the reactions of MTS/PMS agents, and seriously impaired accuracy of cell viability. A different assay, Guave ViaCount,[16, 17] was thus applied here for determination of the cytotoxicity of folate-targeted liposomes against KB and MCF-7 cells. This assay provides repeatable and reliable results[13] although it is much more time-consuming and expensive than the MTS assay.

Cells were first plated in 48-well plates at a density of 30,000-60,000 cells/mL, 0.2 mL per well. After 24 h at 37°C, the media were replaced with drug solutions. Cells were thus incubated with drugs continuously for 72 h, or exposed to drugs for 3 h at 37°C, then washed with PBS x 2 and further incubated up to 72 h in drug-free medium. The same Pt concentrations of aqua-cisPt were used as in f-NB(As, Pt). Cell viability was determined by Guave ViaCount,[13, 16, 17] using a Guava EasyCyte Mini flow cytometer (Guava Technologies, Hayward, CA). Briefly, cells, after released from plates by trypsinization, were stained with the Guava Viacount agent, which contains two fluorescent dyes, one cell permeable and one impermeable. This allows viable and dead cell numbers to be accurately determined by Guava Viacount software. Cell growth rates were expressed as a function of drug concentration on a logarithmic scale. The IC_{50} values (the drug concentration required for 50% inhibition of cell growth) were determined by fitting to a sigmoidal dose-response curve using Origin 6.0 (Microcal Software, Inc., Northampton, USA). The data are shown in Figure 5 and Table 2.

Confocal Microscopy for Visualization of Cellular Liposome Uptake
Cells were first plated, 24-48 h before each experiment, on 22-mm coverslips inside 6-well plates. Cells were then exposed to rhodamine (Rh)-labeled liposomes at 37°C for 3 h at a lipid concentration of 40 μM and an arsenic concentration of 24 μM. After drug-containing medium removal, cells were washed with PBS x 4 and fixed with PBS-buffered 4% paraformaldehyde at 20°C for 5 min, then washed with PBS x 1. Next, the coverslips were mounted on slides coated with PBS. Microscopic visualization of cells was performed using a Zeiss confocal laser scaning microscope (Carl Zeiss LSM 510, Jena, Germany). For rhodamine (Rh), maximum excitation was obtained from the 543-nm line of a He-Ne laser, and fluorescence emission intensities > 570 nm were observed using a long-pass barrier filter LP-570. A water immersion objective, C-Apochromat 63 x 1.2 W corr. (Zeiss), was used. Cells were also imaged by light microscopy using differential interference contrast (DIC). The data are shown in Figures 5a-d.

Quantitative Analysis of Drug Uptake
Cells were first plated, 24 h before each experiment, in 6-well plates with 500,000 cells per well. Cells were then exposed to 10 μM arsenic as free drug or within liposomes for 3 h at 37°C. The same Pt concentration (8 μM) of aqua-cisPt were used as in f-NB(As, Pt). After washing with PBS to remove non-associated drugs, cells were released from tissue culture plates with 0.05% trypsin/0.02% EDTA (Invitrogen), followed by 3 x PBS washing (centrifugation, 500 g, 5 min, 4°C). Two control samples were taken for cell number determination with the Guava ViaCount Assay,[13, 17] using a Guava EasyCyte Mini flow cytometer (Guava Technologies, Hayward, CA). Cell pellets from each well were digested with 100 μL concentrated nitric acid (trace metal grade, Fisher Scientific) for measurement of arsenic (As) and platinum (Pt) concentrations by inductively coupled plasma mass spectroscopy (ICP-MS, X Series II, Thermo Electron, UK). Cell-associated drug was expressed as As and Pt atoms per cell. The data are shown in Figure 5e and Table S2.

Table S2. Comparison of cellular uptake of various drug formulations to tumor cells

Formulations	Cellular uptake (x10^7 atoms/cell)[a]			
	KB (FR$^+$)		MCF-7 (FR$^-$)	
	As	Pt	As	Pt
As$_2$O$_3$	17.1 ± 1.0		9.4 ± 2.3	
NB(As, Pt)	3.2 ± 0.4	0.26 ± 0.06	1.7 ± 0.3	0.18 ± 0.06
f-NB(As, Pt)	131.3 ± 8.1	108.9 ± 18.3	10.2 ± 2.3	7.3 ± 1.7
f-NB(As, Pt) + 2 mM FA	5.8 ± 1.7	1.8 ± 1.4	2.8 ± 1.5	0.7 ± 0.7
Aqua-Pt		0.4 ± 0.1		0.24 ± 0.07

[a] Cellular uptake was measured by ICP-MS after cells were exposed to drugs for 3 h at 37°C. The mean values and standard deviations (± SD) are based on three independent experiments.

Arsenic and Platinum Precipitates from Bulk-Mixed Aqua-cisPt acetate with As(OH)$_3$

5.6 mL of aqua-cisPt acetate (Pt 300 mM, pH 5.1) were mixed with 22.4 mL As$_2$O$_3$ (As 300 mM, pH 12.5). This mixture (As/Pt = 4 mol/mol) was placed into seven falcon-tubes (4 mL/each). The pH of each tube was adjusted from 12.1 to 1.7, 2.6, 3.6, 4.5, 5.5, 6.5, and 8.1, respectively, using HNO$_3$ and NaOH solutions. The tubes were sealed and incubated at 50°C for 4 h and then at 20°C overnight. The pale-yellow precipitate was collected from each tube, washed thoroughly with MQ-H$_2$O and dried over P$_2$O$_5$. The final pH of the supernatant in each tube was measured, and the As/Pt molar ratio of the dried precipitate was determined by ICP-OES in 3% HNO$_3$ (Figure S9). We found lower pH conditions facilitated the precipitate formation at 50°C; when pH > 6.0 (tubes 6 and 7), the amount of precipitate was too small to collect. All precipitates were air stable at room temperature for months, and not soluble in many organic solvents, such as DMSO, DMF, methanol, chloroform, acetone, acetonitrile, benzene, etc. They are sparingly soluble in water, perhaps accompanied by hydrolysis: the starting compounds tend to reform through dissociation of soluble As(OH)$_3$ and cis-[(NH$_3$)$_2$Pt(OH$_2$/OH)$_2$]$^{n+}$ species from the precipitate into water. These precipitates easily dissolve in strong acids and bases (such as 1% HNO$_3$ or HCl, 0.5 M NaOH).
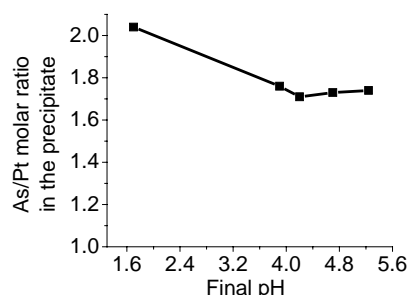

Figure S9. The pH dependence of As/Pt molar ratios in precipitates produced upon mixing aqua-cisPt acetate with As(OH)$_3$ at 50°C, initial As/Pt = 4 mol/mol.

When pH > 3.5, the precipitates had molar ratios of As/Pt less than 2 (Figure S9), likely due to the competitive binding of hydroxide (OH$^-$) towards the Pt centers.[2] When pH > 6, the hydroxo cisPt species became predominant,[18] resulting in significant reduced amounts of arsenic and platinum complexes (Figure S9).[19]

Arsenic and Platinum Nanoparticulates within Liposomes

The dispersion of NB(As, Pt) (20 mL) was centrifuged (2100 g, 30 min, 20°C) to collect liposome nanoparticles. The NB(As, Pt) pellet was re-suspended in 10 mL MQ-H$_2$O and centrifuged at 2100 g for 20 min to pellet liposomes. This washing step (with H$_2$O) was repeated three times for complete removal of soluble salts. The wet liposome pellet was then freeze-dried under high vacuum. Chloroform (8 mL) was added to this dried mixture and the insoluble complex(As, Pt) was collected after centrifugation. This step was repeated 5 times for complete removal of the lipids. The obtained complex(As, Pt)$_{1.36}$ (As/Pt = 1.36 molar ratio) was pale-yellow and stable in air at room temperature for months; it had a similar appearance and physical properties to the precipitates generated by bulk-mixing aqua-cisPt acetate with As$_2$O$_3$ solution at pH 4-5. This powder sample was analyzed by X-ray

photoelectron spectroscopy (XPS) under the Omicron ESCA Probe (Omicron Nanotechnology, Taunusstein, Germany) (Figure S10), and its results were compared with those of As_2O_3, $NaAsO_2$, cisPt, and aqua-cisPt acetate (Table S3). All samples (powder) were embedded into adhesive carbon tapes and mounted in the analysis chamber. The spectra were acquired with X-ray illumination (beam energy 14 eV) under high vacuum (1.0 x 10^{-9} mbar). The surface charge was neutralized with the electron gun. The data were analyzed by the ESI software (Version 2.4, Omicon Nano Technology Ltd., Germany), using the C1s peak (284.8 eV) as calibration reference.[20]
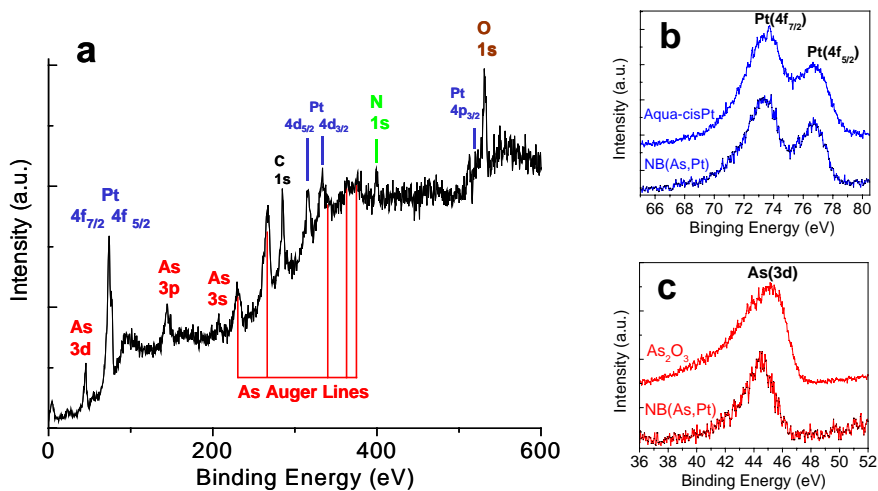

Figure S10. (a) XPS wide scan of complex$(As, Pt)_{1.36}$ separated from NB(As, Pt). The C1s peak is from the carbon tape. XPS narrow region scans of Pt(4f) and As(3d) for complex$(As, Pt)_{1.36}$ from NB(As, Pt) relative to those of aqua-cisPt acetate (b) and As_2O_3 (c).

Table S3. XPS binding energy (eV)[a] of various arsenic and platinum formulations

Formulations	Pt ($4f_{7/2}$)	As (3d)	N1s	O1s
As_2O_3		45.1 ± 0.3 44.9[20]		532.3 531.7[20]
$NaAsO_2$		44.4 ± 0.6 44.2[20]		530.7 ± 0.3
cisPt	73.9 ± 0.01 73.2[20]		400.6 ± 0.6 400.2[20]	
Aqua-cisPt acetate	74.0 ± 0.4		400.7 ± 0.5	531.9 ± 0.5
NB(As, Pt)	73.5 ± 0.4	44.9 ± 0.5	400.4 ± 0.5	531.3 ± 0.3

[a] The values (± SD) of Binding Energy (eV) are based on 2-5 independent experiments.

Since the binding energy of core electrons of an element is sensitive to the chemical environment, the chemical shift of binding energy has been used to study the chemical status of elements,[20] including As[21] and Pt[22] compounds. For NB(As, Pt) (Figure S10 and Table S3), the As(3d) has a binding energy of 45.0 eV with little shift (< 0.5 eV) from those of As_2O_3 and $NaAsO_2$, indicating As atoms remain at As^{III}. For comparison, As^V oxides, such as As_2O_5, have As(3d) at 46-47 eV;[20, 21] intermetallic As^0 compounds, such as AsNb and AsGa, have As(3d) at 40-41 eV.[20] In addition, the Pt($4f_{7/2}$) in NB(As, Pt) has a binding energy of 73.5 eV with little shift (< 0.5 eV) from those of cisPt and aqua-cisPt, indicating Pt atoms remain at Pt^{II}. For comparison, Pt^{IV} compounds, such as $Pt(NH_3)_6Cl_4$ and K_2PtCl_6, have Pt($4f_{7/2}$) at 75-77 eV;[20] Pt^0 compounds, such as PtSn[23] and PtPd,[24] have Pt($4f_{7/2}$) at 70-71 eV.

The complex(As, Pt) formed within liposomes had an As/Pt molar ratio of 1.3 ± 0.1 (n = 7), less than that (1.7 ± 0.1) in the precipitate from bulk-mixing As(OH)$_3$ with aqua-cisPt acetate under the similar conditions in absence of lipids (Figure S9). The extent of arsenic loading and association to Pt appeared to be limited by the barrier of liposome membranes. Although the solid complex(As, Pt) tends to hydrolyze when pH > 6.0 (Figure S9), it becomes less sensitive to extraliposomal pH once sequestered within the liposome (Figure S3). The acidic

intraliposomal conditions (pH 5.1) is likely to be maintained, since the transmembrane pH gradient is difficult to change when the liposome system lacks an effective agent to facilitate proton transport from the internal to the external medium.[25]

X-ray Absorption Spectroscopy (XAS) Analysis on NB(As, Pt)

Aqueous NB(As, Pt) samples were loaded into Lucite cuvettes with 40 μm Kapton windows and rapidly frozen in liquid nitrogen. As K-edge and Pt L_{III}-edge XAS data were collected at Stanford Synchrotron Radiation Laboratory (SSRL) on beamline 9-3 (3 GeV, ~90 mA), using a fully-tuned Si(220) double-crystal monochromator with a Rh-coated mirror upstream of the monochromator for harmonic rejection. As K-edge spectra were measured at 12 K using 10 eV increments in the pre-edge region (11635-11845 eV), 0.35 eV for the edge region (11845-11895 eV), and 0.05 Å^{-1} increments for the extended x-ray absorption fine structure (EXAFS) region (1.45 – 16.0 Å^{-1}), with integration times of 1 s in the pre-edge and edge regions and 5-25 s (k^3 weighted) in the EXAFS region for a total scan time of ~42 min. Pt L_{III}-edge data were measured at 13 K using 10 eV increments in the pre-edge region (11335-11545 eV) , 0.5 eV for the edge region (11545-11595 eV), and 0.05 Å^{-1} increments for the EXAFS region (1.77 – 8.5 Å^{-1}), with integration times of 1 s in the pre-edge and edge regions and 5 s (k^3 weighted) in the EXAFS region for a total scan time of ~10 min. The truncated k-range over which the Pt L_{III} edge EXAFS data was collected is due to the overlap of the Pt L_{III} EXAFS with the As K edge at 11867.0 eV (Pt L_{III} k = 8.63 Å^{-1}).

Pt L_{II} XAS data were recorded at SSRL on beamline 7-3, using a fully-tuned Si(220) double-crystal monochromator with a Rh-coated mirror upstream of the monochromator for harmonic rejection.. The sample temperature was held at 8.5 K in an Oxford liquid He flow cryostat during data collection. Pt L_{II}-edge spectra were measured at 7 K using 10 eV increments in the pre-edge region (13040-13250 eV), 0.35 eV for the edge region (13250-13300 eV), and 0.05 Å^{-1} increments for the EXAFS region (1.62 – 12.0 Å^{-1}), with integration times of 1 s in the pre-edge and edge regions and 20 s (k^3 weighted) in the EXAFS region for a total scan time of ~ 30 min. For all samples (on both beamlines), incident intensity was measured using an N_2-filled ion chamber and energy calibration was performed using foils as internal standards, with the first inflection point of the As foil K-edge spectrum defined as 11867 eV, the first inflection point of the Pt foil L_{III}-edge spectrum defined as 11563 eV, and the first inflection point of the Pt foil L_{II}-edge spectrum defined as 13272.3 eV.

As K-edge XAS data were collected as fluorescence excitation spectra using a thirty-element Ge solid-state detector array, equipped with a 6 μm Ge filter and Soller slits focused on the Ge detector. The integrated count rate for each channel held below ~90 kHz to avoid detector saturation. The windowed As Kα count rates were ~ 19 – 20 kHz in the EXAFS region, giving a total of ~ 1.3×10^7 – 1.4×10^7 useful counts per scan at k = 16 Å. For all samples, each channel of each scan was examined independently for glitches and good channels (27 per scan) were averaged to give the final spectrum. Average files for the As K-edge data of NB(As, Pt) samples were calculated using 7 scans.

Pt L_{III}-edge XAS data were collected as fluorescence excitation spectra using a thirty-element Ge solid-state detector array, equipped with a 6 μm Ge filter and Soller slits focused on the Ge detector. The Ge filter absorbs the elastic scatter while transmitting the Pt fluorescence signal. The integrated count rate for each channel was held below ~90 kHz to avoid detector saturation. The windowed Pt Lα$_1$ count rates were ~ 7.9 – 15.6 kHz in the EXAFS region, giving a total of ~ 1.1×10^6 – 2.2×10^6 useful counts per scan k = 8.5 Å^{-1}. Measurements were truncated at k ~ 8.5 Å^{-1} due to the presence of the As K edge. For all samples, each channel of each scan was examined independently for glitches and good channels (27 per scan) were averaged to give the final spectrum. Average files for the Pt L_{III}-edge data of NB(As, Pt) samples were calculated using 15 scans.

Pt L_{II}-edge XAS data were collected as fluorescence excitation spectra using a thirty-element Ge solid-state detector array, equipped with a 3 μm Zn filter and Soller slits focused on the Ge detector. The Zn filter absorbs both the elastic scatter and the As Kα emission while transmitting the Pt Lα fluorescence. The integrated count rate for each channel was held below ~90 kHz to avoid detector saturation. The windowed Pt Lα$_1$ count rates were ~ 4.8 kHz in the EXAFS region, giving a total of ~2.7×10^6 counts per scan at k = 12 Å^{-1}. Because a significant fraction of the Lα fluorescence originates from excitation of the L_{III} rather than the L_{II} edge, only a fraction of these counts are useful for the L_{II} EXAFS (i.e., there is a much larger than normal background signal, thus accounting for the higher noise level of these spectra). For all samples, each channel of each scan was examined independently for glitches and good channels (27 per scan) were averaged to give the final spectrum. Average files for the Pt L_{II}-edge data of NB(As, Pt) samples were calculated using 21 scans.

X-ray absorption near-edge structure (XANES) data (not shown) were normalized by fitting data to the McMaster absorption coefficients below and above the edge using a single background polynomial and scale factor.[26, 27] The

EXAFS background correction for both As K-edge and Pt L_{II} and L_{III}-edge was performed by fitting a three-region cubic spline for all samples. The data were then converted to k-space using $E_0 = 11887$ eV for As, and $E_0 = 13292.3$ eV for Pt. Fourier transforms were calculated using k^3 weighted data over ranges of 3.5-15.1 Å^{-1} (for the As XAS data) and 2.6-10.5 Å^{-1} (for the Pt XAS data). EXAFS data can be described by the following equation:

$$\chi(k) = \sum_s \frac{N_s S_s(k) A_s(k)}{k R_{as}^2} \exp\left(-2k^2 \sigma_{as}^2\right) \exp\left(\frac{-2R_{as}}{\lambda}\right) \sin\left(2kR_{as} + \phi_{as}(k)\right),$$

where $\chi(k)$ is the fractional modulation in the absorption coefficient above the edge; N_s is the number of scatters at a distance R_{as}; $A_s(k)$ is the backscattering amplitude; σ_{as}^2 is the root-mean-square variation in R_{as}; $\phi_{as}(k)$ is the phase shift experienced by the photoelectron wave in passing through the potentials of the absorbing atom; λ is the mean free path of the photoelectron and backscattering atoms; and $S_s(k)$ is a scale factor specific to the absorber-scatterer pair. The sum is taken over all scattering interactions.[28] The program Feff version 7.02[29] was used to calculate amplitude and phase functions, $A_s(k)\exp(-2R_{as}/\lambda)$ and $\phi_{as}(k)$ for As-O and Pt-O/N interactions at 2.0 Å, and Pt-As and As-As interactions at 3.0 Å. Data were analyzed in k-space using the program EXAFSPAK.[30] For all data, S_s was fixed at 0.9 based on fits to the EXAFS data for structurally characterized model complexes.[31, 32]

For As, the data can only be fit using two shells of scatters, one at ~1.7 Å and one at ~2.3 Å, representing As-O and a heavier scatterer, respectively. The ~2.3 Å shell could, in principle, be due to As-As, although there is no precedent for arsenic oxides with such a short distance. However, fits with As-As are 5-fold worse than fits with As-Pt (Tables S4-5). There are additional outer-shell interactions that can be seen in the Fourier transform (Figure 2g); interpretation of these features will be presented at a later time.

For Pt, the fitting is somewhat ambiguous due to the limited k range. The Fourier transform of the L_{III} edge data shows two higher-R shoulders on the main peak, suggesting that there are three unresolved shells of nearest neighbors. Consistent with this, fits using 3 shells (Pt-O/N + Pt-As + Pt-O/N) were attempted. The large peak at ~ 1 Å in the Fourier transform of the L_{III} edge data is an artifact of the incomplete background removal that results from such a limited k range. Because the Pt L_{II} data was measured to a higher k than the Pt L_{III} data (Figure S11a), the L_{II} data (while noisy) gave more stable fitting results. Therefore, the L_{II} data was used to obtain fitting parameters that could be fixed in the fits of the L_{III} data. Fits of the L_{II} data yielded Pt-O/N distances consistent with a four-coordinate Pt complex, a Pt-As distance consistent with the As K-edge data, and reasonable Debye-Waller factors. Coordination numbers were constrained to chemically reasonable values. Fits of the L_{III} data, with Debye-Waller factors and coordination numbers constrained to those of the Pt L_{II} EXAFS fit, gave distances consistent with the other data collected. Because of the limited k-range, it is difficult to distinguish between Pt-As and Pt-Cl scattering based solely on the EXAFS; however, Cl was removed by metathesis with silver acetate, as confirmed by XPS, thus ruling out Pt-Cl scattering as the source of the ~2.3 Å Pt-X interaction. The near identity of the Pt-As distance (from the Pt L_{II} EXAFS) and the As-Pt distance (from the As EXAFS) confirms that this interaction is due to a novel Pt-As covalent bond.

Based on these fits and literature precedents, the structure illustrated in Figure S11b is proposed. An alternative structure of di-hydroxo/oxo-bridged dinuclear [Pt(μ-O/OH)$_2$As] would not accommodate the very short Pt-As distance (~2.3 Å) and As-O and Pt-N/O geometrical restraints. According to literature,[33] the shortest M-M distances in di-hydroxy/oxo bridged metal centers are over 2.5 Å. These considerations, plus the structurally established precedents of Pt^{II}-As^{III} Lewis adducts mentioned in the main-text lead us to favor the model shown in Figure S11b. We tentatively assign the third shell in the Pt EXAFS to Pt-O(arsenite) scattering.

Table S4. EXAFS (As-K edge) fitting results for NB(As, Pt)

edge	N_{idp}[a]	N_{var}	First Shell: O/N			Second Shell: Pt			ΔE_0	ξ'[b]
			CN	R (Å)	$\sigma^2 \times 10^3$	CN	R (Å)	$\sigma^2 \times 10^3$		
As K	14.77	6[c]	3.3	1.718	2.3	1	2.325	1.7	-11.5	31.8
k = 3.5 – 15.1			First Shell: O/N			Second Shell: As				
R = 0.8 – 2.8			CN	R (Å)	$\sigma^2 \times 10^3$	CN	R (Å)	$\sigma^2 \times 10^3$	ΔE_0	ξ'
		6	3.5	1.741	2.5	1	2.313	1.6	-1.68	153

[a] N_{idp} is the number of independent data points in the region of the Fourier transformed spectrum where the data are physically meaningful. The equation $N_{idp} = (2\Delta k \Delta R)/\pi$ yields N_{idp} as a conservative estimate for all above samples.

[b] ξ', mean-square deviation between the k^3-weighted data and fit divided by (N_{idp}–N_{var}), where N_{var} is the number of variables in the fit. ξ' values provide a partial correction for the fact that more parameters invariably give better fits. Ref [32].

[c] fitting parameters that were varied are denoted in italics.

Table S5. EXAFS (Pt-L$_{II}$ and Pt-L$_{III}$ edge) fitting results for NB(As, Pt)

edge	N_{idp}[a]	N_{var}	First Shell: O/N			Second Shell: As			Third Shell: O			ΔE_0	ξ'[b]
			CN	R (Å)	$\sigma^2 \times 10^3$	CN	R (Å)	$\sigma^2 \times 10^3$	CN	R (Å)	$\sigma^2 \times 10^3$		
Pt L$_{II}$	10.07	7[c]	3	1.977	3.1	1	2.308	1.6	3	3.587	8.7	-12.0	186.8
k = 2.6 – 10.5													
R = 0.8 – 2.8													
Pt L$_{III}$	7.45	4[c]	3	1.996	3.1	1	2.321	1.6	3	3.636	8.7	-10.3	29.5
k = 2.5 – 8.35													
R = 0.8 – 2.8													

[a] N_{idp} is the number of independent data points in the region of the Fourier transformed spectrum where the data are physically meaningful. The equation $N_{idp} = (2\Delta k \Delta R)/\pi$ yields N_{idp} as a conservative estimate for all above samples.

[b] ξ', mean-square deviation between the k^3-weighted data and fit divided by (N_{idp}–N_{var}), where N_{var} is the number of variables in the fit. ξ' values provide a partial correction for the fact that more parameters invariably give better fits. Ref [32].

[c] fitting parameters that were varied are denoted in italics.

[d] the Debye-Waller factors of the Pt L$_{III}$ EXAFS fits were constrained to the values obtained from the Pt L$_{II}$ EXAFS fit.
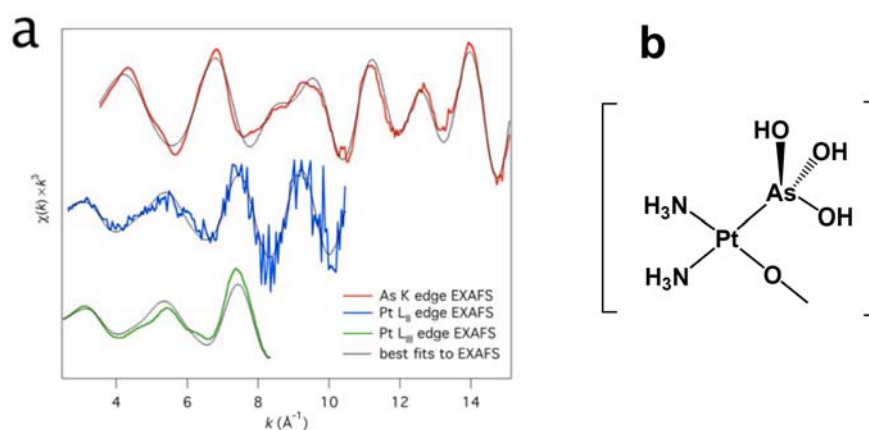
Figure S11. (a) EXAFS spectra and corresponding best fits for NB(As, Pt). Spectra are offset for comparison. (b) Possible interaction between As(OH)$_3$ and aqua-cisPt within liposomes.

References

[1]   A. Gabizon, A. T. Horowitz, D. Goren, D. Tzemach, F. Mandelbaum-Shavit, M. M. Qazen, S. Zalipsky, *Bioconjug. Chem.* **1999**, *10*, 289-298.

[2]   T. G. Appleton, R. D. Berry, C. A. Davis, J. R. Hall, H. A. Kimlin, *Inorg. Chem.* **1984**, *23*, 3514-3521.

[3]   R. C. MacDonald, F. D. Jones, R. Qiu, *Biochim Biophys Acta* **1994**, *1191*, 362-370.

[4]   H. Chen, R. C. MacDonald, S. Li, N. L. Krett, S. T. Rosen, T. V. O'Halloran, *J. Am. Chem. Soc.* **2006**, *128*, 13348-13349.

[5]   G. Haran, R. Cohen, L. K. Bar, Y. Barenholz, *Biochim Biophys Acta* **1993**, *1151*, 201-215.

[6]   N. J. Burger Koert, W. H. M. Staffhorst Rutger, C. de Vijlder Hanke, J. Velinova Maria, H. Bomans Paul, M. Frederik Peter, B. de Kruijff, *Nat Med* **2002**, *8*, 81-84.

[7]   B. A. Lewis, D. M. Engelman, *J. Mol. Biol.* **1983**, *166*, 211-217.

[8]   F. C. Meldrum, V. J. Wade, D. L. Nimmo, B. R. Heywood, S. Mann, *Nature* **1991**, *349*, 684-687.

[9]   T. Douglas, M. Young, *Nature* **1998**, *393*, 152-155.

[10]   T. M. Allen, P. Sapra, E. Moase, *Cell. Mol. Biol. Lett.* **2002**, *7*, 889-894.

[11]   J. M. Saul, A. Annapragada, J. V. Natarajan, R. V. Bellamkonda, *J. Controlled Release* **2003**, *92*, 49-67.

[12]   F. Sonvico, C. Dubernet, V. Marsaud, M. Appel, H. Chacun, B. Stella, M. Renoir, P. Colombo, P. Couvreur, *J. Drug Del. Sci. Tech.* **2005**, *15*, 407-410.

[13]   H. Chen, R. Ahn, J. V. d. Bossche, D. H. Thompson, T. V. O'Halloran, *Mol. Cancer Ther.* **2009**, 8(7).

[14]   R. J. Lee, P. S. Low, *J. Biol. Chem.* **1994**, *269*, 3198-3204.

[15]   B. K. Sekhon, R. H. Roubin, A. Tan, W. K. Chan, D. M.-Y. Sze, *Assay Drug Dev. Technol.* **2008**, *6*, 711-721.

[16]   D. Stearns, A. Chaudhry, T. W. Abel, P. C. Burger, C. V. Dang, C. G. Eberhart, *Cancer Res.* **2006**, *66*, 673-681.

[17]   M. Donaldson, A. Antignani, J. Milner, N. Zhu, A. Wood, L. Cardwell-Miller, C. M. Changpriroa, S. H. Jackson, *Cell Death Differ* **2009**, *16*, 125-138.

[18]   S. J. Berners-Price, T. A. Frenkiel, U. Frey, J. D. Ranford, P. J. Sadler, *J. Chem. Soc., Chem. Commun.* **1992**, 789-791.

[19]   O. M. Ni Dhubhghaill, P. J. Sadler, *Struct. Bonding (Berlin)* **1991**, *78*, 129-190.

[20]   W. F. S. J. F. Moulder, P. E. Sobol, K. D. Bomben, *Handbook of X-ray Photoelectron Spectroscopy* Physical Electronics, Inc., Minnesota, USA, **1995**.

[21]   D. Atzei, S. Da Pelo, B. Elsener, M. Fantauzzi, F. Frau, P. Lattanzi, A. Rossi, *Ann. Chim.* **2003**, *93*, 11-19.

[22]   J. W. Keister, J. E. Rowe, J. J. Kolodziej, T. E. Madey, *J. Vac. Sci. Technol. (B)* **2000**, *18*, 2174-2178.

[23]   J. M. Ramallo-Lopez, G. F. Santori, L. Giovanetti, M. L. Casella, O. A. Ferretti, F. G. Requejo, *J. Phys. Chem. B* **2003**, *107*, 11441-11451.

[24]   J. Pollmann, R. Franke, J. Hormes, H. Bonnemann, W. Brijoux, A. Schulze Tilling, *J. Electron Spectrosc. Relat. Phenom.* **1998**, *94*, 219-227.

[25]   T. E. Redelmeier, L. D. Mayer, K. F. Wong, M. B. Bally, P. R. Cullis, *Biophys. J.* **1989**, *56*, 385-393.

[26]   W. H. McMaster, N. K. Del Grande, J. H. Mallet, J. H. Hubbell, **1969**, (Commerce, U. S. D. o., Ed.).

[27]   T. C. Weng, G. S. Waldo, J. E. Penner-Hahn, *J. Synchrotron Radiat.* **2005**, *12*, 506-510.

[28]   B. K. Teo, *EXAFS: Basic Principles and Data Analysis*, New York, **1985**.

[29]   S. I. Zabinsky, J. J. Rehr, A. Aukudinov, R. C. Albers, M. J. Eller, *Phys. Rev. B: Condens. Matter* **1995**, *52*, 2995-3009.

[30]   G. N. George, I. J. Pickering, **1993**, Stanford University, Palo Alto, CA.
[31]   C. P. McClure, K. M. Rusche, K. Peariso, J. E. Jackman, C. A. Fierke, J. E. Penner-Hahn, *J. Inorg. Biochem.* **2003**, *94*, 78-85.
[32]   K. Clark-Baldwin, D. L. Tierney, N. Govindaswamy, E. S. Gruff, C. Kim, J. Berg, S. A. Koch, J. E. Penner-Hahn, *J. Am. Chem. Soc.* **1998**, *120*, 8401-8409.
[33]   L. Que, Jr., W. B. Tolman, *Angew. Chem., Int. Ed.* **2002**, *41*, 1114-1137.